Two-Phase Flow Phenomena with Depressurization—Consequences for the Design and Layout of Safety and Pressure Relief Valves

Phänomene zweiphasiger Strömung bei Druckentlastung—Folgerungen für Konstruktion und Auslegung von Sicherheits- und Druckentlastungsventilen

F. MAYINGER

Lehrstuhl A für Thermodynamik, Technische Universität München, Postfach 20 24 20, 8000 Munich (F.R.G.)

Abstract

Depressurization through safety and pressure relief valves has gained increasing interest in safety strategies for chemical plants. A best-estimate design of these valves needs reliable information on various thermohydraulic phenomena.

Flashing and phase separation in saturated liquids and vapour–liquid mixtures are very complicated thermodynamic and fluid-dynamic processes, as discussed in this paper. The critical flow through the valve is a function of the inlet conditions, mainly pressure and void fraction, and of the thermodynamic properties. There is still some disagreement in the literature whether and to what extent slip between the phases influences the critical mass flow rate. Finally, two-phase flow friction in the pipes and in the valve itself can control the mass flow rate during depressurization considerably. In pipes of very large diameter reliable measurements on two-phase friction are still lacking.

Kurzfassung

Hochdruckentspannung über Sicherheits- und Druckentlastungsventile gewann zunehmendes Interesse bei sicherheitstechnischen Überlegungen für chemische Anlagen. Eine physikalisch reale Auslegung dieser Ventile benötigt zuverlässige Informationen über verschiedene thermohydraulische Phänomene.

Entspannungsverdampfung und Phasenseparation in gesättigten Flüssigkeiten sowie in Dampf–Flüssigkeits-Gemischen sind sehr komplizierte thermo- und fluiddynamische Prozesse, was in diesem Aufsatz dargelegt wird. Die kritische Strömung durch das Ventil ist eine Funktion der Zulaufbedingungen, hauptsächlich des Druckes und des Dampfgehaltes und der thermodynamischen Eigenschaften. In der Literatur herrscht immer noch Uneinigkeit darüber, ob und in welchem Maße Schlupf zwischen den Phasen den kritischen Massenstrom beeinflußt. Schließlich bestimmt der zweiphasige Reibungsdruckverlust in den Rohren und im Ventil selbst den Mengenstrom in erheblichem Maße während der Druckentlastung. Für Rohre sehr großen Durchmessers fehlen bis heute zuverlässige Messungen über den zweiphasigen Druckverlust.

Synopse

Die Auslegung von Sicherheits- und Druckentlastungsventilen chemischer Anlagen war und ist von gewissen Unsicherheiten behaftet, die bereits daher rühren, daß die Entspannungsverdampfung, das Aufschäumen und die Phasenseparation bisher theoretisch schwer zugänglich sind. Diese drei Prozesse bestimmen aber den Zustand des zweiphasigen Gemisches und *dessen zeitliche Änderung am Eintritt der Zuleitung zum Druckentlastungs- bzw. Sicherheitsventil.*

Bei der Druckentlastung kann man die in Abb. 1 skizzierten Phänomene beobachten. Es bilden sich in der Flüssigkeit Blasen aus, deren erster Entstehungsort dort zu beobachten ist, wo die höchste Keimzahl vorhanden ist, also z.B. an einer Heizfläche oder auch an der Behälterwand. Da die Unterdruckwelle viel rascher fortschreitet, als sich die Blasenbildung

ausbreiten kann, entsteht häufig eine Übersättigung in der Flüssigkeit. Mit fortschreitender Zeit schäumt das Gemisch auf, wobei der Anstieg der Gemischspiegelhöhe eine Funktion des sich abbauenden Siedeverzugs und der Phasenseparation ist.

Das Zusammenspiel zwischen dem nach dem Siedeverzug sich wieder einstellenden thermischen Gleichgewicht und der Phasenseparation, d.h. der Geschwindigkeit, mit der sich der gebildete Dampf von der Flüssigkeit lösen und aufschwimmen kann, beeinflußt den Druckverlauf im Behälter, wie Abb. 2 zeigt. Man erkennt dort am Anfang der Druckentlastung einen raschen Druckabfall (Periode B–C) und durch Vergleich der Temperaturaufzeichnung wird deutlich, daß diese Periode durch eine Überhitzung der Flüssigkeit, zunächst ohne Dampfbildung, gekennzeichnet ist.

In der anschließenden Periode zwischen C und D bildet sich ein Dampfflüssigkeitsgemisch aus und der Gemischspiegel bewegt sich nach oben, bis er schließlich zum Zeitpunkt D den Druckbehälterdeckel erreicht. Mit Einsetzen der Blasenbildung durch Entspannungsverdampfung baut sich die Überhitzung der Flüssigkeit rasch ab. Dabei ist aber zu Beginn (Periode D–F) die Volumenzunahme des Gemisches durch Dampfbildung größer als die Abströmung durch das Ventil. Dies führt zu einem kurzzeitigen Druckanstieg in der Entlastungsphase, wie man ebenfalls aus Abb. 2 erkennt. Schließlich überwiegt die Ausströmung und der Druck klingt asymptotisch ab.

Bei geringen Füllständen steigt der Gemischspiegel nicht so stark an und der zeitliche Druckverlauf ist monoton abfallend, wie man aus Abb. 3 erkennt.

Für das in der allerersten Druckentlastungsphase sich ausbildende thermische Ungleichgewicht und den daraus resultierenden zeitlichen Siedeverzug gibt es nur wenige theoretische Ansätze in der Literatur. Ein Beispiel für einen solchen Ansatz zur Berechnung der Siedeverzugszeit, wie ihn Kantrowitz [4], Probstein [5] und Collins [3] vorschlugen, zeigt Gl. (1).

Für die Phasenseparation von Dampf und Flüssigkeit gibt es eine Reihe von Veröffentlichungen in der verfahrenstechnischen und auch in der kerntechnischen Literatur. Die Phasenseparation und die daraus resultierende mittlere Dichte des Gemisches im Behälter wird meist als Funktion der Froude-, der Weber- und der Bond-Zahl dargestellt. Viecenz [1] entwickelte, gestützt auf eigene Messungen und aufbauend auf die Angaben in der Literatur, eine eigene Beziehung (Gl. (7)), die zusätzlich noch den Einfluß der Viskositäten der Phasen berücksichtigt. Daraus läßt sich dann auch die Geschwindigkeit der Phasenseparation (Gl. (8)) und die sogenannte Driftgeschwindigkeit ableiten (Gl. (9)).

In den meisten Fällen wird bei der Druckentlastung die ausströmende Menge von der kritischen Geschwindigkeit im engsten Querschnitt des Ventils bestimmt. Die Literatur über thermohydraulische Untersuchungen zur Sicherheit von Kernreaktoren weist eine Vielzahl von Ansätzen für die Berechnung dieser kritischen Geschwindigkeit auf. Die kritische Geschwindigkeit von Gas–Flüssigkeits-Gemischen ist im Gegensatz zu Gasströmungen nicht mit der Schallgeschwindigkeit zahlenmäßig gleich. Die Schallgeschwindigkeit in zweiphasigen Gemischen (Gl. (16)) wird zur Ausbreitung der Druckwellen für Festigkeitsüberlegungen benötigt und ist im wesentlichen eine Funktion des volumetrischen Dampfgehaltes. Für die Berechnung der ausströmenden Menge unter kritischen Bedingungen kann man daraus einen Ansatz (Gl. (17)) ableiten, der den auf die Masse bezogenen Dampfgehalt, dessen Änderung mit der Druckabsenkung, die Kompressibilität der gasförmigen und der flüssigen Phase und die Änderung des Schlupfes zwischen den Phasen mit dem Druck enthält. Der Schlupf wird meist in Form des Dichteverhältnisses zwischen den Phasen (Gl. (18)) dargestellt. Bis zur Formulierung einer Gleichung, wie sie zum Beispiel von Moody (Gl. (19)) angegeben wurde, ist es jedoch noch ein langer Weg, der unter anderem auch Überlegungen zur Energiedissipation und damit zur Entropieänderung erfordert.

Bei engen Zu- und Ableitungsquerschnitten zu bzw. vom Ventil kann aber auch der Reibungsdruckverlust in diesen Rohren die ausströmende Menge begrenzen. Es sind heute verschiedene empirische Korrelationen verfügbar, die den Druckverlust zweiphasiger Gemische in Kanälen zuverlässig vorhersagen lassen und die auf einigen tausend Versuchsergebnissen basieren. Wesentlich weniger ist bekannt über den Druckverlust im Ventil selbst; empirische Gleichungen lehnen sich meist an Ansätze für einphasiges Fluid an und enthalten—wie Gl. (21)—Korrekturen für die zweite Phase.

Eine zuverlässige Vorhersage des Druckentlastungsvorganges erfordert noch Experimente und theoretische Analysen auf verschiedenen Gebieten, insbesondere aber über das Aufschäumen von Mehrstoff-Gemischen mit leichtersiedenden Komponenten sowie den kritischen Massenstrom und den Druckverlust in Ventilen.

1. Introduction

Pressure relief and safety valves have to be designed for a flow rate which guarantees that no inadmissible pressure increase occurs in the case of an accidental transient, like an uncontrolled heat addition or exothermal reaction. If a pressure relief valve protects a vessel which is filled with a liquid partially evaporating during the depressurization, there may be a two-phase mixture—gas and liquid—flowing in the valve.

The flow behaviour of this mixture differs from that of a single-phase component and is strongly dependent on the amount of liquid carried in the gas or vapour flow.

The composition of the vapour–liquid mixture not only influences the pressure drop but also the maximum flow rate, the so-called critical flow, in the valve. As a consequence, the momentum forces downstream of the valve also depend on this two-phase quality. In practice it is frequently usual to assume pure vapour flow in the valve, from a conservative point of view, to

be sure that the desired velocity of depressurization is reached and to be on the safe side of the position of the narrowest cross-section in the valve. In such a case inadmissible momentum forces can occur if the valve is exposed to two-phase flow instead of the assumed pure vapour flow, and the unnecessary fast depressurization can create pressure or shock waves in the vessel, damaging installations there.

To know the flow conditions in the valve, we have to learn about evaporation, phase separation and entrainment in the vessel and on the way to the valve during the depressurization.

Owing to a boiling delay the liquid will not evaporate instantaneously when the depressurization starts and, because of this, a large thermodynamic disequilibrium can occur, with the consequence of an explosive-like evaporation after this delay, which produces more vapour than the safety or pressure relief valve can release. For this reason, the pressure may even recover again for a short period.

2. Phenomena during depressurization

During the discharge of a pressure vessel we can observe the phenomena represented qualitatively in Fig. 1. We shall assume that the vessel is filled with a liquid under saturation before the depressurization starts (Fig. 1(a)). When the pressure decreases, vapour bubbles are created in the liquid. Where this bubbling is initiated depends on the presence of nuclei in the liquid. In the absence of nuclei the bubble formation starts from the upper surface of the liquid and travels downward, due to a mass-transfer-like process, because a part of the bubbles created in an upper layer acts as nuclei for a lower one. This progress of the nucleation or evaporation front is much lower than the sonic velocity, with which the depressurization wave travels through the liquid. So in the lower part of the liquid a rather large thermodynamic disequilibrium can be built up, before it is reached by the nucleation front.

If nuclei of vapour bubbles are present in the vessel, for example in wall roughnesses or due to a heat-ing process, the evaporation starts where these nuclei are highly concentrated.

This flashing evaporation increases the volume of the fluid in the vessel and the level of the fluid, called the swell level, rises. Simultaneously droplets are formed above this swell level, owing to the penetration of vapour bubbles through the upper surface of the mixture. These droplets, however, can also be created by the expansion of the vapour being originally above the liquid, as we can easily understand if we remember the path of an isentropic curve near the saturation line.

The further movement of the swell level then strongly depends on the relative velocity between the vapour bubbles and the liquid. This relative velocity is a function of the thermodynamic properties, like surface tension and viscosity, as well as of the temporal course of the depressurization. If the vapour bubbles could rise freely and separate completely from the liquid, the swell level would not reach the upper end of the vessel. With a fast depressurization the phase separation is too small, however, which means that more vapour is formed than can escape through the liquid and thus the mixture foams strongly and expands. This is mainly the case after the boiling delay, when the liquid evaporates explosively. In this way, a two-phase mixture can reach the nozzle at the upper end of the vessel and, through the connecting pipe, the safety or pressure relief valve.

The temporal course of this evaporation and the rising of the swell level influences the depressurization, as shown qualitatively in Fig. 2. Refrigerant R12 was used in the experiments [1] as the test fluid, from which the results of Fig. 2 are taken. The vessel in this experiment was filled up to two-thirds of its height by liquid before the depressurization started, during which the pressure was lowered from 20 bar to ambient pressure within 15 s. The depressurization was initiated at the moment B, as indicated in Fig. 2, and the rapid pressure decrease from B to C, together with the reading from the temperature curve in Fig. 2, show that during this period the liquid is superheated owing to a boiling delay. The line in the temperature curve of Fig. 2 indicated by an arrow is the saturation line. So
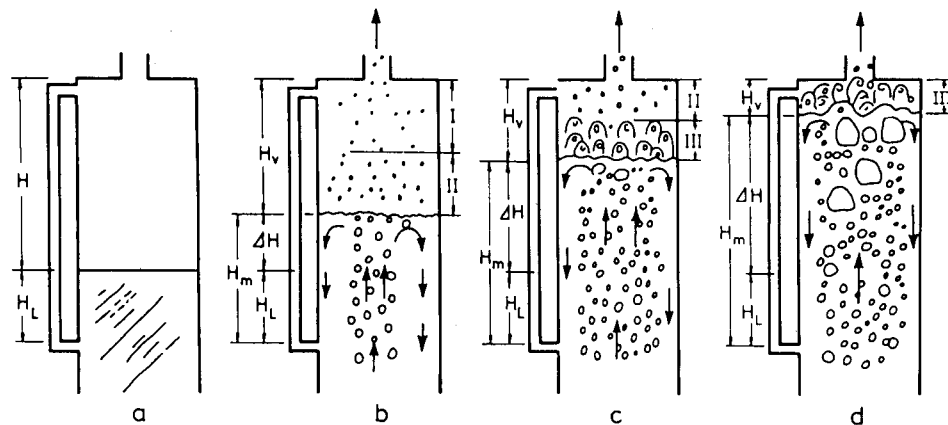

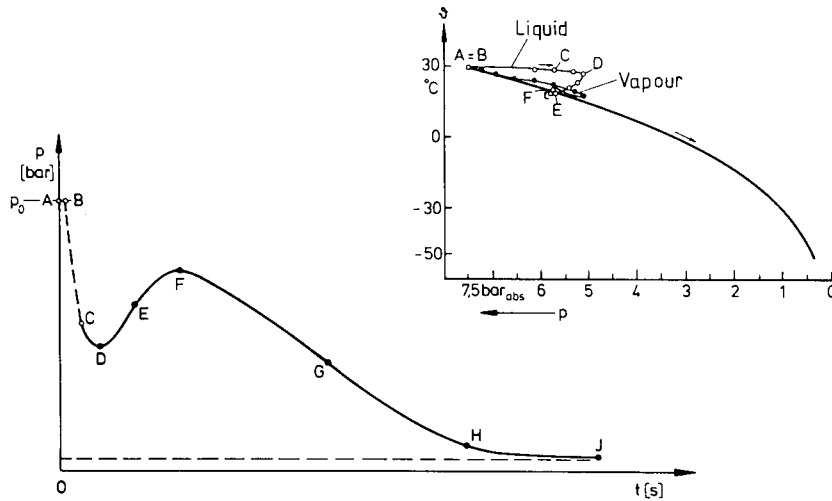Fig. 1. Flashing and two-phase flow phenomena with depressurization.

Fig. 2. Thermodynamic disequilibrium during depressurization.

all thermodynamic conditions above this saturation line are of superheated nature.

So, at the very beginning mainly the vapour dome above the liquid level is expanding, and only at the moment C flashing evaporation, and thus bubble formation, start in the liquid. During the period C–D the swell level moves upward, as briefly explained above, until it reaches the nozzle of the vessel leading to the pressure relief valve, which is the moment D in Fig. 2. Then the flow conditions in the valve change, because now the fluid entering the valve is a two-phase mixture instead of vapour carrying some droplets, as it was before. Approximately in the same moment, however, the high superheating in the liquid decreases rapidly and so the vapour production in the vessel during the period D–F is larger than the volume flowing through the valve. In this connection we also have to remember that the volumetric flow rate of a vapour–liquid mixture is smaller than that of pure vapour.

Both phenomena result in an increase of the pressure until the moment F, when the vapour production just equals the volumetric flow rate through the valve. Finally, the pressure in the vessel can decrease again and the pressure–time curve flattens when the swell level falls below the outlet nozzle.

With constant thermodynamic initial conditions this pressure increase after the first depressurization depends on the initial liquid level in the vessel. With low liquid levels the mixture cannot swell up to the outlet nozzle and there is only a slight change of slope on the pressure–time curve, as Fig. 3 indicates [1]. With high initial levels and a vessel filled up almost to the outlet nozzle, the pressure increase after the first depressurization at the very beginning is strongly marked.

The formation of the swell level is a strong function of the surface tension and the viscosity of the liquid also has some influence. Fast depressurization promotes the swelling.

At a given pressure difference between inlet and outlet of the valve the volumetric flow rate diminishes with increasing liquid content in the vapour. Here,
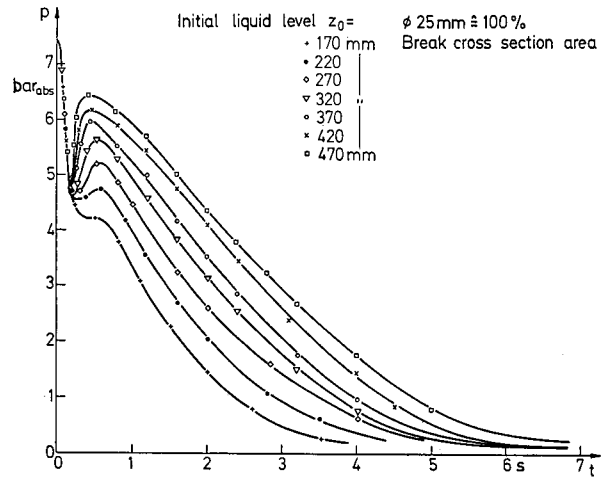

Fig. 3. Influence of the filling situation on phase separation and swelling.

however, we have to realize that in most situations the pressure drop in the valve is so large that critical flow conditions occur. The critical mass flow rate increases with decreasing quality, that is, with decreasing vapour content. Owing to the high pressure drop in the valve, flashing evaporation is present there too, which also influences the mass flow rate.

So the temporal depressurization of a vessel is a rather complicated interaction between flashing evaporation, phase separation and critical mass flow rate. To predict the depressurization and to design a pressure relief valve reliably, we need precise information about these phenomena.

3. Boiling delay

During a fast depressurization the liquid will not form gaseous nuclei and flash exactly at the moment when the pressure falls below the saturation pressure, but the liquid will become superheated and will reach a metastable thermodynamic state. The thermody-

namic disequilibrium and thus the extent of superheating depend on the number and character of nuclei in the vessel. Roughnesses and cavities in the walls of the vessel can act as nuclei; gaseous enclosures in the form of very tiny bubbles or clusters of highly activated molecules can also initiate flashing.

In multi-component mixtures the more volatile component could produce nuclei for flashing, because during the temporal course of depressurization the pressure at first falls short of its saturation condition. In a homogeneous fluid and under the transient conditions of a depressurization the probability of nuclei formation is an exponential function of the number of more volatile molecules, the diffusion coefficient and the time, according to Zeldovich [2]. A similar theory was given by Collins [3]: he introduced the activation energy and the product of Boltzmann constant and temperature to express the probability of nuclei formation and, from this, to develop a theory for predicting the boiling delay. From the theories of Zeldovich and Collins a formula can be derived for the so-called relaxation time, which gives the period needed to reach equilibrium after the saturation pressure falls. According to Kantrowitz [4], Probstein [5] and Collins [3], this relaxation time can be expressed in the form

$$\tau = \frac{2\pi kT}{D\gamma} = \frac{2\pi R_e^2 \rho_v}{Bm} \left(\frac{kT}{\sigma}\right)^{1/2} \quad (1)$$

where B is a kinetics term, D the diffusion coefficient, R_e the critical radius of the nuclei, k the Boltzmann constant, T the temperature, m the mass of a molecule, ρ_v the density of the vapour, γ the second derivative of the work needed to form the nucleus, and σ the surface tension.

Up to now no reliable correlation for predicting the relaxation time or boiling delay in technical systems is known. The only information which can be drawn from experiments is the hint that the boiling delay is of the order of a few hundredth to several tenths of a second.

It has to be pointed out that assuming instantaneous nucleation during depressurization—zero boiling delay—does not give results which are on the conservative side in technical calculations, because with increasing boiling delay the flashing is more and more explosive-like, and so the real thermodynamic and fluid-dynamic conditions at the relief valve can differ considerably from those which were predicted when neglecting boiling delay. Much more fundamental and applied research work is needed to get at least a rough idea of boiling delay in real single- and multi-component fluids.

4. Phase separation

The interaction between phase separation and vapour production controls the swell level. It seems to be obvious and easy to formulate the phase separation by describing the rising velocity of the vapour bubbles in the liquid. This rising velocity is controlled by the buoyancy and by the drag of the bubbles in the liquid.

For a given relative velocity between the bubble and the liquid the latter one, that is, the flow resistance, is a function of the viscosity of the liquid and of the size of the bubble, which in its turn depends on the surface tension. Attempts to describe the phase separation by formulating the rising velocity of a single bubble and adding correction factors, taking into account the interaction within the bubble swarm, failed. Therefore, in the literature it has become usual to express the phase separation in the form of a mean void fraction

$$\langle \epsilon \rangle = \frac{V_G}{V_G + V_L} \quad (2)$$

in the vessel by using empirical correlations, based on similarity deliberations and dimensionless numbers. Examples of such correlations are given in Table 1. These correlations commonly contain three dimensionless numbers, namely the Froude number

$$\mathrm{Fr} = \frac{w_{G,0}^2}{g[\sigma/g(\rho_L - \rho_G)]^{1/2}} \quad (3)$$

the Weber number

$$\mathrm{We} = \frac{g[\sigma/g(\rho_L - \rho_G)]^{1/2}}{d_{\mathrm{Vess}}} \quad (4)$$

and the Bond number

$$\mathrm{Bo} = g d_{\mathrm{Vess}}^2 \frac{\rho_L - \rho_G}{\sigma} \quad (5)$$

In these equations the indices G and L refer to the gas or vapour phase and the liquid phase, respectively. For simplicity, a fictive vapour velocity, namely the velocity $w_{G,0}$ which the vapour would have if it flowed alone in the vessel, is used in the Froude number. The characteristic length in the Weber and in the Bond number is the diameter of the vessel, d_{Vess}. With this fictive velocity $w_{G,0}$ the mean rising velocity of the bubbles can easily be calculated by simply using

$$w_{G,0} = \langle \bar{\epsilon} \rangle \bar{w}_{\mathrm{Bub}} \quad (6)$$

A comparison of results calculated with the formulae in Table 1 and experimental data using different fluids gives satisfactory agreement only within narrow areas and for limited thermodynamic conditions. Viecenz [1] therefore modified these equations and developed one based on his own measurements with the refrigerant R12:

$$\langle \bar{\epsilon} \rangle = C \left\{ \frac{w_{G,0}^2}{g[\sigma/g(\rho_L - \rho_G)]^{1/2}} \right\}^n$$
$$\times \left\{ \frac{[\sigma/g(\rho_L - \rho_G)]^{1/2}}{d_{\mathrm{Vess}}} \right\}^{0.174}$$
$$\times \left(\frac{\rho_L}{\rho_G - \rho_G}\right)^{-0.585} \left(\frac{v_L}{v_G}\right)^{0.256} \quad (7)$$

Equation (7) is formulated with the Froude number, the Weber number and the ratios of densities and viscosities of the phases. The constant C and the exponent n with the Froude number depend on the flow pattern in the vessel. C and n have to be altered if bubbly flow changes into churn flow. This change in

TABLE 1. Empirical correlations for mean void fraction with phase separation

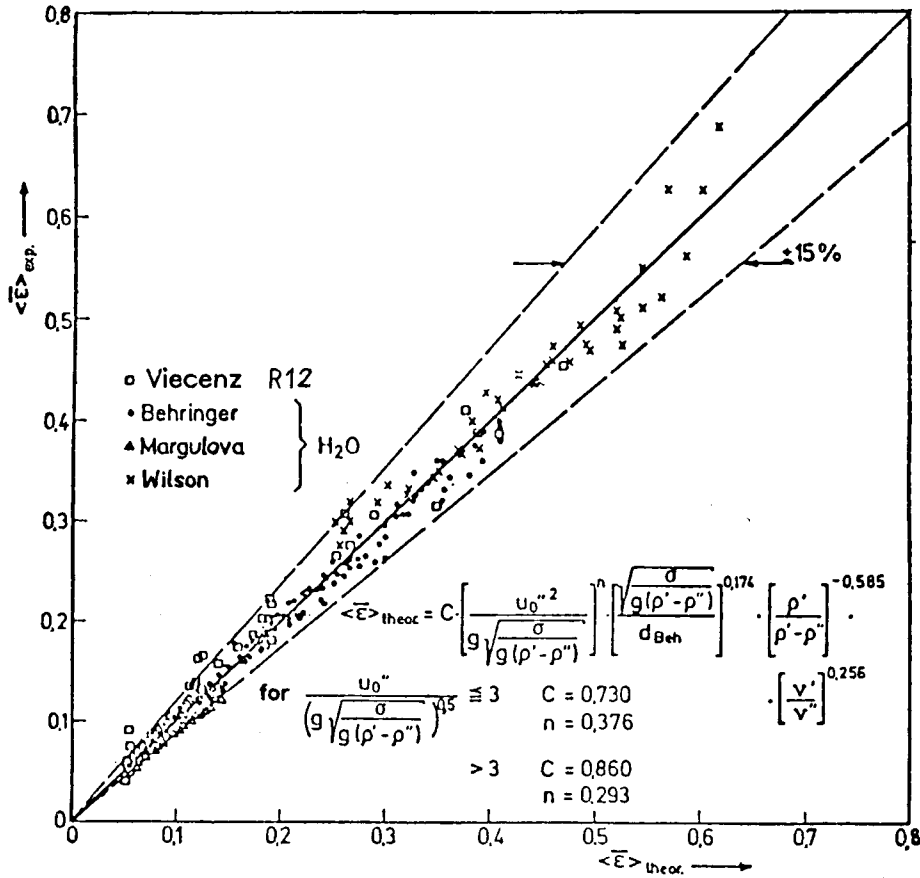| Author	Substance	Geometry/data	Empirical correlation for mean void fraction		Phase pattern distinction	Pressure ratio
Wilson [6]	H_2O–H_2O vapour	d_{vess} 480 mm 100 mm Sint. plate	$\langle\bar\epsilon\rangle = C(\mathrm{Fr})^a(\mathrm{We})^{0.1}\left(\dfrac{\rho_G}{\rho_L-\rho_G}\right)^{0.17}$	$C = 0.68$ $a = 0.31$ $C = 0.88$ $a = 0.20$	$\dfrac{w_{G,0}}{\sqrt{g[\sigma/g(\rho_L-\rho_G)]^{1/4}}} \leqslant 2$ $\dfrac{w_{G,0}}{\sqrt{g[\sigma/g(\rho_L-\rho_G)]^{1/4}}} > 2$	20–41
Sterman Dementiev Lepilin [7]	H_2O–H_2O vapour	d_{vess} 51 mm 69 mm 85 mm Evaporator Sint. plate	$\langle\bar\epsilon\rangle = C(\mathrm{Fr})^a(\mathrm{We})^{0.25}\left(\dfrac{\rho_G}{\rho_L-\rho_G}\right)^{0.17}$	$C = 1.07$ $a = 0.40$ $C = 1.90$ $a = 0.17$	$\dfrac{w_{G,0}}{\sqrt{g[\sigma/g(\rho_L-\rho_G)]^{1/4}}} < 3.7$ $\dfrac{w_{G,0}}{\sqrt{g[\sigma/g(\rho_L-\rho_G)]^{1/4}}} \geqslant 3.7$	1.07–190
Margulova [8]	H_2O–H_2O vapour	d_{vess} 200 mm Sint. plate	$\langle\bar\epsilon\rangle = (0.576+0.00414p[\mathrm{atm}])w_{G,0}^{0.75}$		No	91–190
Kurbatov [9]	H_2O–H_2O vapour	d_{vess} 51–200 m Evaporator Sint. plate	$\langle\bar\epsilon\rangle = 0.67(\mathrm{Fr})^{1/3}(\mathrm{We})^{1/6}\left(\dfrac{\rho_L}{\rho_L-\rho_G}\right)^{1/3}\left(\dfrac{v_L}{v_G}\right)^{2/9}$		No	1.07–190
Labuncov		d_{vess} 17–748 mm	$\langle\bar\epsilon\rangle = \left(1+\dfrac{w_{Bub}}{w_{G,0}}\right)^{-1}$ $\qquad w_{Bub,\infty} = 1.5\left[\dfrac{g\sigma(\rho_L-\rho_G)}{\rho_L^2}\right]^{1/4}$ $\psi_L = 1.5\left(\dfrac{\rho_L}{\rho_G}\right)^{1/5}\left(1-\dfrac{\rho_G}{\rho_L}\right)^5$ $w_{Bub} = w_{Bub,\infty}\psi_L$		Bo > 500	1–196
Mersmann [11]	Air–H_2O H_2O–Hg Toluol–H_2O		$\langle\bar\epsilon\rangle(1-\langle\bar\epsilon\rangle)^n = 0.14 w_{G,0}\left(\dfrac{\rho_L^2}{g\sigma(\rho_L-\rho_G)}\right)^{1/4}$ $\times\left(\dfrac{\rho_L}{\rho_L-\rho_G}\right)^{1/3}\left[\dfrac{\sigma^3\rho_L^2}{\eta_L^4(\rho_L-\rho_G)g}\left(\dfrac{\rho_L}{\rho_G}\right)^{5/3}\right]^{1/24}$		$n = f\left(\dfrac{\rho_L}{\rho_G}\right)$	

Fig. 4. Void fraction with phase separation: comparison of literature data.

the flow pattern can easily be expressed by the Froude number. With $Fr \leqslant 3$ bubbly flow prevails and $C = 0.73$ and $n = 0.376$ have to be used. With $Fr > 3$ there is mainly churn flow in the vessel and $C = 0.86$ and $n = 0.293$ must be used.

Viecenz [1] compared his equation with experimental data from the literature, using mainly water and also refrigerant R12 as test fluids and found good agreement, as Fig. 4 demonstrates.

The prediction of the phase separation becomes much more difficult during depressurization, because here the foaming of the mixture due to flashing evaporation and the movement of the swell level have to be taken into account. The vapour volume per unit area per unit time separating out of the mixture, which because of its dimensions $m\ s^{-1}$ is also called the mean separation velocity $\bar{w}_{sep}$, is a function of the drift velocity w_{drift}, the mean void fraction described in eqn. (7) and a radial distribution factor $C_{0,\,rad}$ of the void in the vessel. The velocity of the swell level surface has also to be taken into account. For the separation velocity, which is the volumetric flow rate of vapour per unit area per unit time out of the mixture, we can write

$$w_{sep} = \frac{w_{G,\,0}C_{0,\,rad}\langle\bar{\epsilon}\rangle}{1 - C_{0,\,rad}\langle\bar{\epsilon}\rangle} + \frac{w_{drift}\langle\bar{\epsilon}\rangle}{1 - C_{0,\,rad}\langle\bar{\epsilon}\rangle} - w_{surf}\langle\bar{\epsilon}\rangle \quad (8)$$

and for the drift velocity w_{drift} Viecenz [1] found

$$w_{drift} = 0.2591 \left[\frac{g\sigma(\rho_L - \rho_G)}{\rho_G{}^2}\right]^{1/4} \left(\frac{\rho_G}{\rho_L - \rho_G}\right)^{0.4755}$$

$$\times \left[\frac{g\sigma/(\rho_L - \rho_G)}{d_{Vess}}\right]^{-0.3064} \left(\frac{v_L}{v_G}\right)^{-0.3405}$$

$$\times \left[\frac{H_L}{\sigma/g(\rho_L - \rho_G)}\right]^{0.0778} \quad (9)$$

The radical distribution parameter $C_{0,\,rad}$ was finally defined by Viecenz as

$$C_{0,\,rad} = C[\langle\bar{\epsilon}\rangle]^a \left(\frac{\rho_G}{\rho_L - \rho_G}\right)^b \quad (10)$$

In eqn. (9) H_L is the height of the liquid in the vessel before depressurization starts. The constants and exponents of eqn. (10) are given in Table 2. Use of eqn. (8) presupposes a very complicated and detailed analysis of bubble formation during the flashing

TABLE 2. Constants and exponents in eqn. (10)

	C	a	b
$\langle\bar{\epsilon}\rangle < 0.104$	1.783	-0.242	0.142
$0.104 \leqslant \langle\bar{\epsilon}\rangle < 0.24$	2.20	-0.143	0.147
$\langle\bar{\epsilon}\rangle \geqslant 0.24$	1.0	0	0

evaporation, including information on the boiling delay and the recovery of the thermodynamic equilibrium, because these phenomena control the velocity of the swell level surface, w_{surf}. An attempt at such an analysis is given in ref. 1.

5. Critical flow

The velocity with which pressure and density waves travel through compressible substances is called the sonic velocity a. Using the conservation laws for mass, energy and momentum and assuming isentropic pressure fluctuations, we get for the sonic velocity a the well-known equation

$$a = \left(\frac{dp}{d\rho}\right)_s^{1/2} \tag{11}$$

The index s in this equation means constant entropy. Using the equation of state of an ideal gas—the so-called Boyle–Mariott law—we can formulate the maximum or critical velocity in short nozzles:

$$w_{crit} = (\kappa p_s v_s)^{1/2} = (\kappa R T_s)^{1/2} \tag{12}$$

which, for an ideal gas, is identical with the sonic velocity, that is, the travelling velocity of a small pressure perturbation.

For two-phase mixtures we have to be careful when defining a sonic velocity, because from a microscopic point of view the travelling velocity of a pressure perturbation is different in areas occupied by vapour and by liquid. Also, the critical velocity w_{crit} does not give comprehensive information, because to predict the critical mass flow rate we have to know the mean density of the void fraction. Defining the mean density of a vapour–liquid mixture as

$$\bar{\rho} = \epsilon \rho_G + (1 - \epsilon)\rho_L \tag{13}$$

we can rewrite eqn. (11) in the form

$$a_{2\,ph}^2 = \frac{dp}{d[\epsilon \rho_G + (1 - \epsilon)\rho_L]} \tag{14}$$

Finally, by using the relationship between the so-called slip ratio $k = w_G/w_L$, the quality $\dot{x} = \dot{M}_G/(\dot{M}_G + \dot{M}_L)$ and the void fraction ϵ,

$$k = \frac{\dot{x}}{1 - \dot{x}} \frac{1 - \epsilon}{\epsilon} \frac{\rho_L}{\rho_G} \tag{15}$$

we can rewrite eqn. (13) in the form

$$a_{2\,ph}^2 = \left\{\left[\epsilon^2 + \epsilon(1 - \epsilon)\frac{\rho_L}{\rho_G}\right]\frac{d\rho_G}{dp}\right.$$
$$+ \left[(1 - \epsilon)^2 + \epsilon(1 - \epsilon)\frac{\rho_G}{\rho_L}\right]\frac{d\rho_L}{dp}$$
$$+ (\rho_G - \rho_L)\frac{1 - \epsilon}{\dot{x}(1 - \dot{x})}\frac{d\dot{x}}{dp}$$
$$\left. - \epsilon(1 - \epsilon)(\rho_G - \rho_L)\frac{dk}{dp}\right\}^{-1} \tag{16}$$

From this equation we can see that the travelling velocity of sonic waves in a two-phase mixture is a function of the compressibility of the vapour and of the change of quality $\dot{x}$ and slip ratio k with pressure.

In a similar way we can derive an equation for the critical mass flow rate $\dot{m}_{crit}$:

$$\dot{m}_{crit}^2 = -\left\{k\left[[1 + \dot{x}(k - 1)]\dot{x}\frac{dv_G}{dp}\right.\right.$$
$$+ \{v_G[1 + 2\dot{x}(k - 1)]$$
$$+ k v_G[2(\dot{x} - 1) + k(1 - 2\dot{x})]\}\frac{d\dot{x}}{dp}$$
$$+ k[1 - \dot{x}(k - 2)$$
$$- \dot{x}^2(k - 1)]\frac{dv_L}{dp} + \dot{x}(1 - \dot{x})$$
$$\left.\left. \times \left(kv_L - \frac{v_G}{k}\right)\frac{dk}{dp}\right]^{-1}\right\} \tag{17}$$

Also the critical mass flow rate is a function of the compressibility of the phases and of the quality and slip gradient in the orifice valve where critical velocity occurs.

Theoretical models existing in the literature differ mainly in the method by which they describe the change of quality and of slip ratio, as can be seen, for example, in refs. 12–14. There are two limits from the thermodynamic point of view, namely total thermodynamic disequilibrium (so-called frozen flow) or fully thermodynamic equilibrium due to sufficient flashing in the orifice. On the fluid-dynamic side, equal velocity of vapour and liquid ($k = 1$) can be assumed, or a simple slip model can be used. Moody [12], for example, calculates the slip in the orifice during critical flow only as a function of the densities of liquid and vapour:

$$k = \left(\frac{\rho_L}{\rho_G}\right)^{1/3} \tag{18}$$

In other models, instead of the cubic root the square root is used.

Moody started his theoretical deliberations from the fact that the mixture in the orifice is expanding isentropically, but he assumed thermodynamic equilibrium. From the balance equations for mass, energy and momentum he derived for the critical mass flow the equation

$$\dot{m}_{crit, Moody} = \left[\frac{2(h_0 - h_L - h_{LG})}{(s_0 - s_L)s_{LG}}\right]^{1/2}$$
$$\times \left[\frac{k(s_G - s_0)v_L}{s_{LG}} + \frac{(s_0 - s_L)v_G}{s_{LG}}\right]^{-1}$$
$$\times \left(\frac{s_0 - s_L}{s_{LG}} + \frac{s_G - s_0}{k^2 s_{LG}}\right)^{-1/2} \tag{19}$$

In this equation h_0 and s_0 stand for the specific enthalpy or specific entropy under stagnation conditions, that is, before the fluid is accelerated and depressurized; h_{LG} and s_{LG} are the latent heat of evaporation and the entropy change during this evaporation.

The assumption concerning the behaviour of the slip ratio in the nozzle influences the calculated value
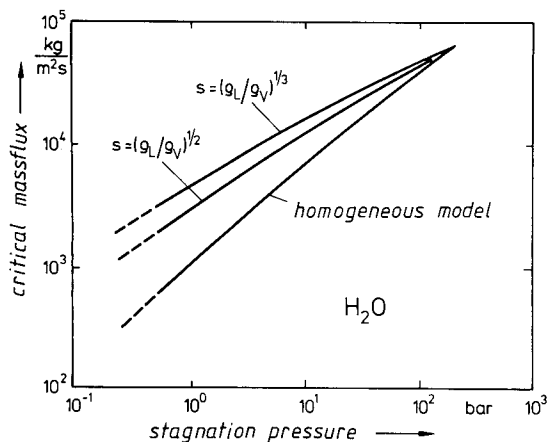
Fig. 5. Influence of slip behaviour on critical mass flow.

of the critical mass flow rate quite considerably, as Fig. 5 points out.

The homogeneous model, assuming equal velocity of the phases and fully developed thermodynamic equilibrium, predicts the lowest critical mass flow rates and frozen flow gives the highest values.

The critical mass flow also depends, however, on the geometrical shape of the nozzle itself. Short orifices (especially with single-phase fluids under stagnation conditions) produce a much higher critical flow rate than nozzles with a length over diameter ratio of more than 10. The prediction of critical mass flow rate in pressure relief or safety valves is still more difficult and unreliable, because they are much more complicated flow ducts than are simple orifices or nozzles. If the fluid has to pass through a long tube behind the orifice or valve, it undergoes an additional pressure drop which may become so large that it is an additional or even the only limitation for the mass flow rate. The critical mass flow rate strongly decreases with quality $\dot{x}$, and the pressure drop increases rapidly with quality. So, critical mass flow rate conditions may occur in the tube following the nozzle, or the pressure drop in the tube may limit the maximum flow. For a more reliable layout of depressurization components we therefore have to know the friction pressure loss in the valve and in the tubing, too.

6. Friction pressure loss

Equations and methods for predicting friction pressure loss in tubes and ducts of different cross-section are well known from the literature. However, no systematic research has been performed up to now on pressure loss in valves. Empirical correlations in the literature are usually based on a few experiments under very special conditions only. A good survey of the literature on pressure loss in fittings is given by Friedel [15]. The empirical and semi-empirical models in the literature can be divided into homogeneous and heterogeneous ones. The homogeneous models [16, 17] assume equal velocity between the phases. The heterogeneous models [18–21] either propose simple slip

models, or a proper slip model has to be taken from the literature. Chisholm [18], for example, takes into account different slip behaviour of the vapour–liquid mixture by adjusting coefficients in his equation. In the models of Morris [20] and of Simpson et al. [21] simple slip correlations are integrated in the model. Heckle [22] distinguishes between flow conditions and, depending on the flow pattern, he proposes the use of homogeneous or heterogeneous treatment.

Homogeneous models are only valid for special flow patterns, like fog flow or dispersed bubbly flow. With heterogeneous models one has to be aware of the fact that they are only as good and reliable as the slip correlation used in them is in predicting the real conditions correctly. These slip correlations are usually only valid for fully developed adiabatic two-phase flow in cylindrical tubes. In fittings the geometrical conditions are much more complicated; the flow is not fully developed and, owing to the large pressure drop, flashing evaporation occurs.

As in cylindrical tubes, the models for predicting the pressure loss in fittings use the two-phase multiplier

$$R = \frac{(\Delta p/\Delta l)_{2\ \text{phase}}}{(\Delta p/\Delta l)_{\text{single phase}}} \tag{20}$$

which connects the pressure loss of the two-phase mixture with that of single-phase flow. This means that as a starting condition a calculation has first to be performed which gives the pressure loss that the value would undergo if there were single-phase flow. For this calculation it is usually assumed that the total mass of the two-phase mixture flows in the liquid state.

Here, as an example, only the correlations by Chisholm [18] will be given:

$$R = 1 + (\rho_L/\rho_G - 1)[B\dot{x} + (1 - B)\dot{x}^2] \tag{21}$$

where

$$B = 0.5, \ 1.5, \ 2.3$$

or

$$B = [1/k + (k - 2)\rho_G/\rho_L]/(1 - \rho_G/\rho_L)$$

For the slip ratio s in this equation, any proper correlation or model from the literature can be taken.

For other models reference is made to the paper by Friedel [15], where a large number of correlations are presented and carefully compared with measured data existing in the literature.

7. Separation of the liquid before or after the depressurization valve

As we have seen, the liquid in the two-phase mixture reduces the volumetric flow rate through the depressurization valve because of the increasing pressure drop. The liquid carries most of the mass flowing out and is the main factor endangering the environment when containing toxic or explosive substances. On the other side the liquid carried out does not contribute to the cooling of the reactive mass in the pressure vessel, but forms outside the safety valve a slowly evaporating
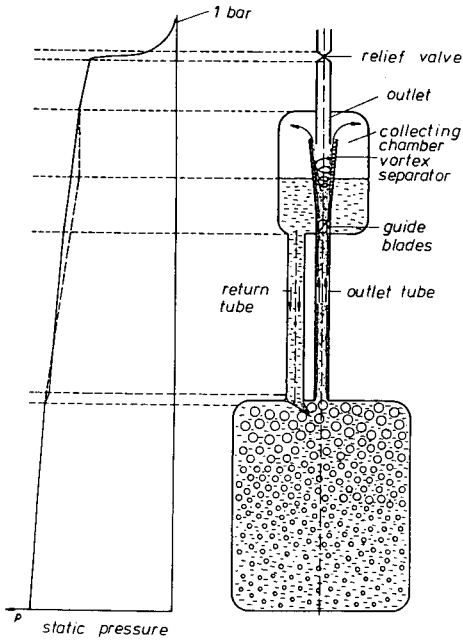
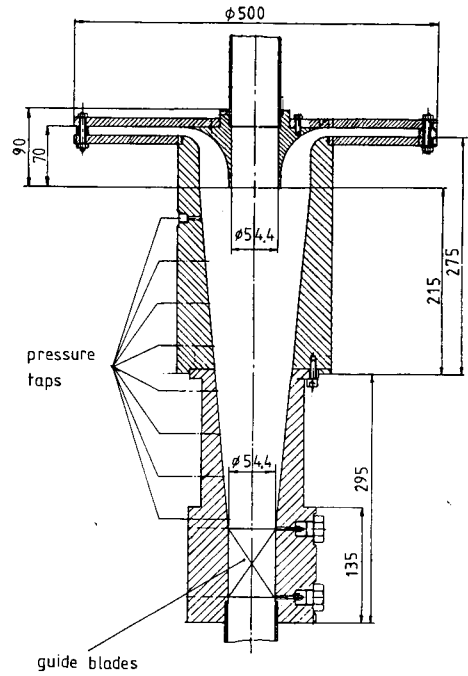Fig. 6. Pressure profile in an external separation device.

Fig. 7. Design for an optimized vortex separator built into a pressure relief unit.

mass producing a highly concentrated atmosphere. Therefore it is advantageous to separate the liquid before entering the pressure relief device and to transport it back to the pressure vessel. To do this a separator of high efficiency and low pressure drop is needed.

A design for a device which could prevent toxic or explosive liquid escapes to the environment in non-allowable amounts is shown in Fig. 6. The separator is positioned at a certain level above the pressure vessel to allow the separated liquid to flow back under gravity into the pressure vessel through a bypass parallel to the blow-down channel. To make this reflux

possible the pressure losses in the blow-down channel including the separator must be smaller than the hydrostatic pressure difference in the reflow bypass. It must be remembered that the separated liquid in the reflow bypass and also in the collecting vessel around the separator will continue to flash during the blow-down and may even still undergo an exothermal reaction. This produces a foaming which reduces the hydrostatic pressure difference.

There are many gas–liquid separators available on the market; however most of them produce too great
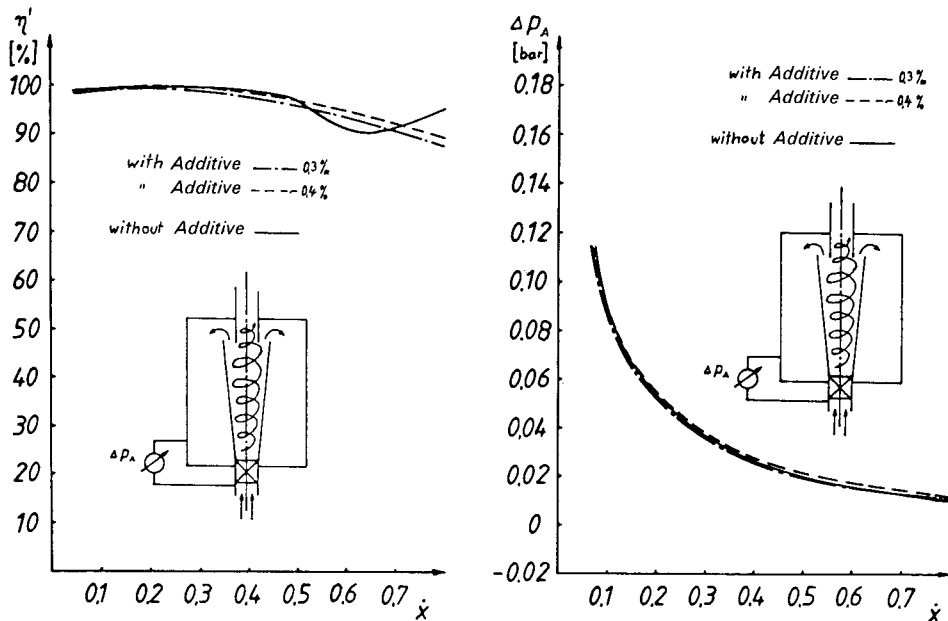

Fig. 8. Separation efficiency (left) and differential pressure (right) of an optimized vortex separator.

a pressure loss to be useful for the above-mentioned device. A survey of separators is given, for example, by Brauer [23] and can also be found in the *Chemical Engineer's Handbook* [24].

The two-phase mixture in the blow-down channel has a high kinetic energy and with not too small a void fraction it exhibits an annular flow pattern. The design and layout of the separator therefore should utilize these two phenomena. A twist or vortex separator, as shown in Fig. 7, with blades at its entrance influencing only the core of the two-phase mixture, not the liquid film at the wall of the annular flow, fits the conditions best. This vortex separator demonstrated [25] that the demand for recharging of the separated liquid into the vessel without any external energy can be satisfied within certain flow conditions. The separator, however, has to be integrated into the pipe between the vessel and the relief valve in a special manner.

This vortex separator has been tested with a water mixture and is presently under investigation in a blow-down channel with flashing refrigerant R12.

The separation efficiency and the pressure loss of such a vortex separator in its optimized design is shown in Fig. 8. It proved to be highly efficient even with foaming additives in the water of these air–water tests. The pressure loss is moderate and can even be reduced by improving the design of the diffusor through which the liquid flows after being separated from the gas or the vapour. Foam producing additives do not have much influence on the pressure loss.

A vortex separator can certainly also be placed after the safety or pressure relief valve. However, then a special vessel is needed in which to collect the separated liquid. One then has to prevent flashing in this special vessel again producing a two-phase mixture which carries liquid to the environment.

8. Conclusions

With the increasing safety consciousness of the public, behaviour in accidents of chemical apparatus and plant needs more and more attention. To prevent invasion of the environment by toxic or explosive substances, retention devices for the blow-down mass must be provided to deal with an overpressurization of a chemical reactor and the layout of these devices requires reliable and precise data of the fluid-dynamic and thermodynamic conditions occurring during a blow-down in all components of the blow-down section.

Part of the knowledge needed can be taken from the experience gained in the research, design, and operation of nuclear power plants. Chemical substances, however, are in many respects different from those of the water used in a nuclear reactor. Therefore, further experiments have to be performed to study the flashing behaviour, phase separation, critical mass flow rate, and two-phase pressure loss of chemical substances. There is an especially great lack of knowledge concerning the flow behaviour in safety valves and pressure relief valves during blow-down of hydrocarbons and other chemical substances.

References

1 H. J. Viecenz, Blasenaufstieg und Phasenseparation in Behältern bei Dampfeinleitung und Druckentlastung, *Dissertation*, Tech. Univ. Hanover, 1980.
2 Y. B. Zeldovich, *Zh. Eksp. Theor. Fiz.*, *12* (1942) 525.
3 F. C. Collins, *Z. Elektrochem.*, *59* (1955) 404.
4 A. J. Kantrowitz, *Chem. Phys.*, *19* (1951) 1097.
5 R. F. Probstein, *J. Chem. Phys.*, *19* (1951) 619.
6 J. F. Wilson, The velocity of rising steam in a bubbling two-phase mixture, *ANS-Trans.*, *5* (1962) 151.
7 L. S. Sterman, The correlation of experimental data for vapour bubbling through a liquid, *Zh. Tech. Fiz.*, *26* (1965) 1519.
8 T. H. Margulova, An experimental investigation of the velocity in bubbling through a layer of water at high pressures, *Trans. Power Inst. M. V. Molotov, Moscow*, *11* (1953) 1.
9 A. V. Kurbatov, The bubbling and the problem of critical loads in steam separators, *Trans. Power Inst. M. V. Molotov, Moscow*, *11* (1953).
10 D. A. Labunzov, *Teploenergetica*, *7* (1960) 76–81.
11 A. Mersmann, Auslegung und Maßstabsvergrößerung von Blasen- und Tropfensäulen, *Chem.-Ing.-Tech.*, *49* (1977) 679–770.
12 F. J. Moody, Maximum flow rate of a single component, two-phase mixture, *J. Heat Transfer*, *87* (1965) 134.
13 R. E. Henry, A study of one- and two-component, two-phase critical flows at low qualities, *ANL-7430*, Argonne Nat. Lab., 1968.
14 R. E. Henry and H. K. Fauske, The two-phase critical flow of one component mixtures in nozzles, orifices, and short tubes, *J. Heat Transfer*, *93* (1971) 179.
15 L. Friedel, Druckabfall in Armaturen bei Zweiphasenströmung, *Preprints, Technik des Gas/flüssig- und der Dreiphasenströmung, Krefeld, 6. und 7. Dez. 1984*, VDI Verlag, Düsseldorf, pp. 101–135.
16 P. E. Tremblay *et al.*, *Can. J. Chem. Eng.*, *52* (1974) 433–437.
17 C. P. Fairhurst, Two-phase flow component loss data, *Process Eng.*, *64* (7) (1983) 34–36.
18 D. Chisholm, *Proc. Inst. Mech. Eng., Part 3C*, *184* (1969/1970) 24–32.
19 Z. Rouhani, *AE-RTV-841*, Atomic Energy Commission, Sweden, 1969.
20 S. D. Morris, *Heat Transfer and Fluid Flow*, Services (HTFS), UKEA, Harwell, U.K., 1983, p. 68.
21 H. C. Simpson, Two-phase flow through gate valves and orifice plates, *Proc. Int. Conf. on Physical Modelling of Multiphase Flow, Coventry, 1983*.
22 M. Heckle, *Chem.-Ing.-Tech.*, *42* (1970) 304–310.
23 H. Brauer, *Grundlagen der Einphasen- und Mehrphasenströmungen*, Verlag Sauerländer, Frankfurt, 1971.
24 R. H. Perry and D. W. Green, *Chemical Engineer's Handbook*, McGraw-Hill, New York, 6th edn., 1984.
25 S. Muschelknautz, *Vorläufiger Abschlußbericht zum AIF-Forschungsvorhaben "Abscheidung von Flüssigkeit aus Dampf und Druckentlastung"*, Inst. Thermodynamik A, Tech. Univ. Munich, 1986.